

Layer-Wise Data-Free CNN Compression

Maxwell Horton, Yanzi Jin, Ali Farhadi, Mohammad Rastegari
 Apple
 {mhorton, yanzi-jin, afarhadi, mrastegari}@apple.com

Abstract

We present a computationally efficient method for compressing a trained neural network without using any data. We break the problem of data-free network compression into independent layer-wise compressions. We show how to efficiently generate layer-wise training data, and how to precondition the network to maintain accuracy during layer-wise compression. Our generic technique can be used with any compression method. We outperform related works for data-free low-bit-width quantization on MobileNetV1, MobileNetV2, and ResNet18. We also demonstrate the efficacy of our layer-wise method when applied to pruning. We outperform baselines in the low-computation regime suitable for on-device edge compression while using orders of magnitude less memory and compute time than comparable generative methods. In the high-computation regime, we show how to combine our method with generative methods to improve upon state-of-the-art performance for several networks.

1. Introduction

Inference with Convolutional Neural Networks (CNNs) is typically computationally expensive [24, 22, 44, 43]. As a result, practical methods for compressing CNNs are of great interest. Application domains involving machine learning on low-power, low-compute devices require efficient CNNs for on-device execution. Examples include smart-home security, factory automation, and mobile applications. One common technique for improving CNN computational efficiency is quantization. In many cases, a CNN with 32-bit weights and activations can be converted to a CNN with a lower-bit representation (*e.g.* 8-bit, 4-bit, or even 1-bit) with little or no loss of accuracy [28, 40, 26]. Another common technique for CNN compression is weight pruning [30, 49, 19, 13]. The removal of network weights allows the network to occupy a smaller memory footprint and achieve a faster execution time.

Most methods for CNN compression require retraining on the original training set to achieve a high compression

rate. Applying post-training quantization usually results in poor network accuracy [26] unless special care is taken in adjusting network weights [40]. Handling low-bit quantization provides additional challenges when data is not available. Popular methods for compressing through sparsity [30, 49, 19, 13] also require training on the original data. Unfortunately, many real-world scenarios require compression of an existing model but prohibit access to the original dataset. For example, data which is legally sensitive, or which has privacy restrictions, may not be easily accessible. In some cases, data may not be available if a model which has already been deployed needs to be compressed.

As CNNs continue moving from cloud computing centers to edge devices, the need for efficient algorithms for compression has also arisen. The increasing popularity of federated learning [37] has increased the importance of on-device algorithms for efficient machine learning. Additionally, models deployed to edge devices may need to be compressed on-the-fly to support certain use cases. For example, models running on edge devices in areas of low connectivity may need to compress themselves when battery power is low. Such edge devices usually do not have enough storage to hold a variety of models with different performance profiles. Thus, we are interested in the problem of data-free model compression in the low-compute setting.

We propose a simple and efficient method for achieving high compression rates for data-free network compression. Our method is a layer-wise optimization based on the teacher-student paradigm [23]. A pretrained model is used as a teacher that will help train a compressed student model. During optimization, we generate data to approximate the input to a layer of the teacher network and use it to optimize the corresponding layer in the compressed student network. Figure 1 illustrates an overview of our method. This layer-wise optimization approach allows us to converge quickly while still maintaining high accuracy, resulting in a significantly more efficient compression process than end-to-end network optimization [15, 53].

Our method can be integrated with any compression scheme for the student network. In this paper, we show how network quantization and weight pruning can be used.

We precondition the network to bring weights across layers to a similar scale, then we use BatchNorm [25] statistics to generate data used for layer-wise quantization and pruning. Our method is orders of magnitude more efficient than comparable generative methods. We achieve state-of-the-art results for data-free quantization of MobileNetV1 [24], MobileNetV2 [45], and ResNet [22] on the challenging ImageNet [9] dataset, even when comparing against high-computation methods. We also outperform computationally efficient baselines for pruning, and improve upon the results of computationally expensive generative methods by combining our method with them.

2. Related Work

Pruning and Quantization: Quantization involves reducing the numerical precision of weights and/or activations from a typical 32-bit floating point representation to a lower-bit integral representation [28, 18, 34, 14, 32]. Methods typically quantize between 8 bits [50, 4, 26, 28, 52] and 1 bit [43, 7, 11, 36]. The most commonly used quantization scheme is affine quantization [26]. Other formulations can include a scale and a zero-point for each channel [28].

Soft Threshold Reparameterization (STR) [30] achieves state-of-the-art results with a simple training technique that increases sparsity as training progresses. Several other works present magnitude-based pruning methods [19, 49, 19, 17, 3, 41]. Alternatives to magnitude-based pruning involve using gradient information [13, 31, 21, 10, 8], covariance information [33], or regularization [35]. Refer to [30] for a comprehensive overview.

Data-Light and Data-Free Compression: A few recent works have explored methods for quantizing a model using little data (“data-light” methods) or no data (“data-free” methods). In the data-light method AdaRound [39], the authors devise a method for optimizing the rounding choices made when quantizing a weight matrix. In the data-free method Data-Free Quantization Through Weight Equalization and Bias Correction (DFQ) [40], the authors manipulate network weights and biases to reduce the post-training quantization error. Other equalization methods tackle data-free quantization, such as Weight Factorization [38].

A few works have explored data-light and data-free pruning. In the data-light method Principle Filter Analysis [47], activation correlations are used to prune filters. An iterative data-free pruning method is presented in Data-Free Parameter Pruning [46], though they only prune fully-connected layers. Optimal Brain Damage [8] and Optimal Brain Surgeon [21] presents results for data-light and data-free pruning for overparameterized networks such as AlexNet [29]. Layer-wise approaches are explored in [12, 16].

Generative Methods for Data-Free Compression: Given a trained model, it’s possible to create synthetic images that match characteristics of the training set’s statistics.

These images can be used to retrain a more efficient model using only another pretrained model. These methods are computationally expensive.

In Deep Inversion (DI) [53], the authors use a pretrained model to generate a dataset used to train a sparse model. To generate the dataset, a noise image is trained to match the network’s BatchNorm [25] statistics, and to look realistic. The authors generate a dataset and use it to train a sparse model using Knowledge Distillation [23]. A similar method appears in The Knowledge Within [20], although their method is data-light rather than data-free.

In Adversarial Knowledge Distillation [6], the authors generate synthetic images for model training using a Generative Adversarial Network (GAN) [15]. The images are used in conjunction with Knowledge Distillation [23] to train a network. Other GAN-based formulations include Generative Low-bitwidth Data Free Quantization [51].

3. Layer-Wise Data-Free Compression

Our method for data-free network compression begins with a fully trained network and creates a compressed network of the same architecture. This is conceptually similar to Knowledge Distillation [23] in that a pretrained “teacher” network is used to train a “student” network. However, Knowledge Distillation requires training data. Previous approaches have addressed this through generating data, as in Adversarial Knowledge Distillation (AKD) [6] and Deep Inversion (DI) [53]. However, these methods are computationally expensive (Figure 2).

We take a simpler approach illustrated in Figure 1. We view each layer of the student as a compressed approximation of the corresponding layer in the teacher. As long as the approximation of each layer is accurate, the overall student network will produce similar outputs to the teacher. This approach is more computationally efficient than other generative methods, since our method does not need to train an input image to produce good training signal at every layer of a network. Instead, we generate inputs separately for each individual layer, which does not require generating realistic images. Our method takes orders of magnitude less time and memory than AKD [6] and DI [53] (Figure 2), converging after only a few minutes.

Our first challenge lies in generating data used to train compressed approximations of the teacher’s layers, which we address in Section 3.1. Our second challenge lies in preconditioning the network to achieve more effective compression, which we address in Section 3.2. We then present our quantization method in Section 3.3 and our pruning method in Section 3.4.

3.1. Layer-Wise Data Generation

We describe our method for generating layer-wise network inputs. We assume the network is composed of blocks

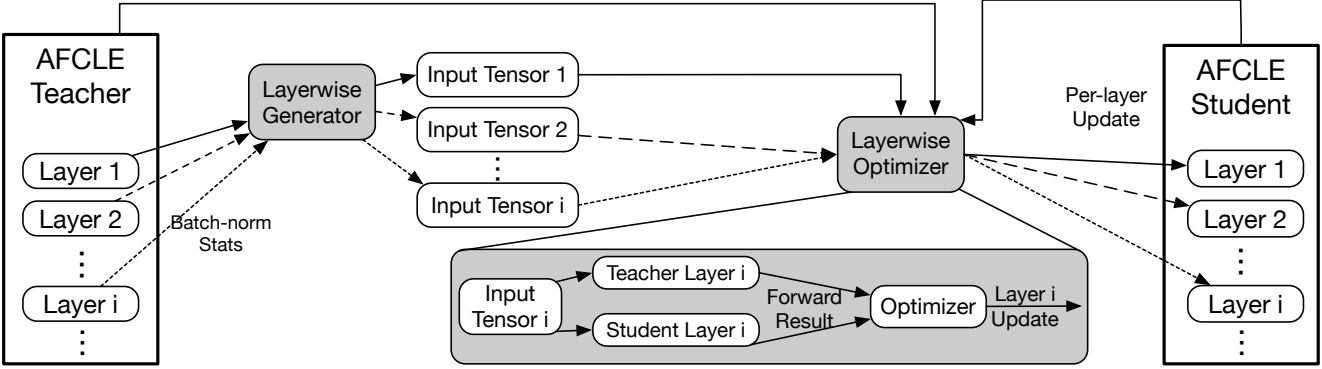


Figure 1. An overview of our method. We first perform BatchNorm fusion and Assumption-Free Cross-Layer Equalization (AFCLE, Section 3.2) on the teacher and student. Then, we train each layer of the student separately. We generate data using BatchNorm statistics from the previous layer (Section 3.1), then use this data to optimize the compressed student network to match the teacher.

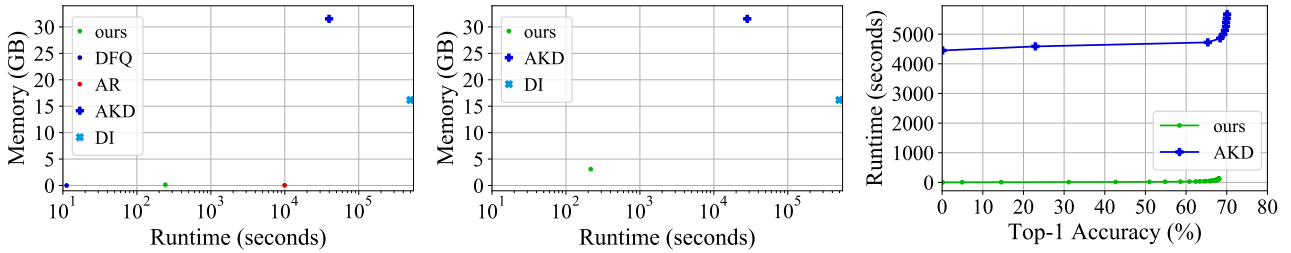


Figure 2. Runtime and memory overhead for quantization and pruning of MobileNetV1 1.0 on ImageNet. To estimate memory overhead, we count the additional memory needed to store buffers for backpropagation (if applicable), plus additional memory needed for the algorithm. Runtime is assessed as the training time needed to achieve within 0.1% of the best accuracy (as well as within 0.1% of the final sparsity level, for pruning jobs). We compare Data-Free Quantization (DFQ) [40], AdaRound (AR) [39], Adversarial Knowledge Distillation (AKD) [6], and Deep Inversion (DI) [53] (some of which are quantization-only methods). **Left:** Quantization to 8 bits. **Middle:** Pruning. **Right:** Accuracy as a function of training time. DI data generation alone (excluding subsequent training) requires 4.92×10^5 seconds of computation so we omit it for clarity.

containing a convolution, followed by a BatchNorm [25], followed by an activation. Let \mathcal{B}_i denote the BatchNorm layer associated with a block of index i . The BatchNorm \mathcal{B}_i normalizes by the mean $\mu_{\mathcal{B}_i}$ and standard deviation $\sigma_{\mathcal{B}_i}$ of its inputs, then applies a channelwise affine transformation with weight $\gamma_{\mathcal{B}_i}$ and bias $\beta_{\mathcal{B}_i}$. Therefore, the standard deviation of the BatchNorm's output channels is $\gamma_{\mathcal{B}_i}$, and the mean of the output channels is $\beta_{\mathcal{B}_i}$.

We exploit this information to generate layer-wise inputs. Let \mathcal{C}_i denote the convolutional layer in block i of the network, and f_i denote the activation in block i . Let $h(\cdot)$ denote the application of layer h to an input.

Consider the case in which block i accepts multiple input tensors from blocks indexed by a collection \mathcal{K} . Let $x_{\mathcal{B}_{i-1}}$ denote the input into the BatchNorm \mathcal{B}_{i-1} from a training batch when training with real data. Assuming these tensors are combined by an addition function (as in Residual Networks [22]), the input $x_{\mathcal{C}_i}$ to convolution \mathcal{C}_i is

$$x_{\mathcal{C}_i} = \sum_{j \in \mathcal{K}} f_j(\mathcal{B}_j(x_{\mathcal{B}_j})). \quad (1)$$

The extension to other combination functions besides addition is straightforward.

When training without data, we do not have access to $x_{\mathcal{B}_j}$, so we estimate it. Let $\mathcal{G}_{\mathcal{C}_i}(\cdot)$ be a function that generates an input used to train layer \mathcal{C}_i . Using our observation above regarding the output statistics of BatchNorm layers, we estimate

$$x_{\mathcal{B}_j} \sim \mathcal{N}(\mu_{\mathcal{B}_j}, \sigma_{\mathcal{B}_j}) \quad (2)$$

$$\mathcal{G}_{\mathcal{C}_i} = \sum_{j \in \mathcal{K}} f_j(\mathcal{N}(\mu_{\mathcal{B}_j}, \sigma_{\mathcal{B}_j})), \quad (3)$$

where $\mathcal{N}(\mu, \sigma)$ denotes a Gaussian function with mean μ and standard deviation σ . If a layer is not preceded by a BatchNorm (as is the case for the first convolutional layer), we generate data from $\mathcal{N}(0, 1)$. We ignore the effect of other layers (such as Average Pooling) on statistics.

We describe how to use this generated data to compute the student network's layers in Section 3.3 and Section 3.4. But first, we describe another component of our method designed to precondition the network to improve final results.

3.2. Assumption-Free Cross-Layer Equalization

We describe our method for equalizing network layers. For ease of notation, $W \in \mathbb{R}^{c_o \times c_i}$ denotes a matrix with c_o output dimensions and c_i input dimensions. The extension of our method to convolutions is straight forward.

Our method breaks the problem of data-free network compression into the subproblem of compressing individual layers. Two issues complicate the matter of assembling a compressed network from compressed individual layers.

The first issue relates to BatchNorm [25] layers. A BatchNorm layer consists of the parameters μ , σ , γ , and β , which correspond to the mean of its inputs, the standard deviation of its inputs, the weight of its affine transformation, and the bias of its affine transformation. Given a linear layer W with bias b , the output of the linear layer, followed by BatchNorm, is

$$f(x) = \frac{Wx + b - \mu}{\sqrt{\sigma^2 + \epsilon}} \odot \gamma + \beta, \quad (4)$$

where ϵ is a small number used to avoid division by 0, and \odot denotes elementwise multiplication [25, 42]. If some row c of W is multiplied by a scale factor a , and if the c^{th} elements of b and μ are multiplied by a , and if the c^{th} element of γ is multiplied by the scalar factor $1/a$, the function $f(x)$ remains unchanged.

Thus, the relative importance of the weights of W depends on the values of BatchNorm parameters. This is problematic when pruning or quantizing W because we want the weight values' magnitudes to reflect their importance. Hidden scale factors inside BatchNorm layers prevent this. To address this, we fuse the BatchNorm parameters μ , σ , γ , and β into the preceding linear layer, so that the BatchNorm parameters' effective influence on weight magnitudes is accounted for. Once this fusion occurs, BatchNorms can be ignored. The BatchNorm statistics used in Equation 3 must be collected before this fusion step. They will remain valid, since the change in BatchNorm parameters is compensated for by the change in W and b .

The second complication with breaking data-free network compression into layer-wise compression subproblems is that the relative magnitude of weights is not calibrated within a single layer. Consider the output of a pair of linear layers with weights W_1 and W_2 , and biases b_1 and b_2 . Suppose the network uses ReLU activations [1], such that the output of the pair of layers is

$$f(x) = \text{ReLU}(W_1(\text{ReLU}(W_2x + b_2)) + b_1). \quad (5)$$

If row c of W_2 is multiplied by a scale factor a , and if the corresponding c^{th} element of b_2 is multiplied by a , and if the corresponding column c of W_1 is multiplied by $1/a$, then output $f(x)$ remains unchanged. In this rescaled network, row c of W_2 has changed, but no other rows in W_2

have changed. Since rows of W_2 can be arbitrarily rescaled in this way, it's possible for a row of W_2 to contain very small values even if the row is important to the network. This is problematic for quantization and magnitude-based pruning.

To address this scaling inconsistency, we employ a method we call Assumption-Free Cross-Layer Equalization (AFCLE), which is an extension of the Cross-Layer Equalization method described in DFQ [40]. With each linear layer \mathcal{L}_j with weight $W_j \in \mathbb{R}^{c_o \times c_i}$ and bias $b_j \in \mathbb{R}^{c_o}$, we associate a pair of vectors, $v_j^i \in \mathbb{R}^{c_j}$ and $v_j^o \in \mathbb{R}^{c_o}$. (The extension to convolutional layers is straightforward.) These vectors will be used during AFCLE, then will remain fixed afterwards. We compute the output of our linear layer as

$$\mathcal{L}_j(x) = (W_j(x \odot v_j^i) + b_j) \odot v_j^o. \quad (6)$$

Before AFCLE, each element of the vectors v_j^i and v_j^o is initialized to 1. Consider a row c of W_2 with weights W_2^c , and a corresponding column c of W_1 with weights W_1^c . We calculate a scale factor s_c , and update the network as

$$s_c = \frac{\sqrt{\max(|W_1^c|) \max(|W_2^c|)}}{\max(|W_2^c|)} \quad (7)$$

$$W_1^c = W_1^c / s_c \quad (8)$$

$$v_1^o = v_1^o * s_c \quad (9)$$

$$b_1 = b_1 / s_c \quad (10)$$

$$W_2^c = W_2^c * s_c \quad (11)$$

$$v_2^i = v_2^i / s_c. \quad (12)$$

Essentially, each v_j^i and v_j^o act as a buffer that records the changes to W_i and b_j , so that we can equalize W_j across layers without changing the network's outputs at any layer. We iterate over all channels and over all pairs of adjacent layers in the network. We continue until the mean of all the scale parameters s_c for one round of equalization deviates from 1 by less than $\epsilon = .001$.

The main difference between our method and Cross-Layer Equalization (CLE) [40] is, our method uses v_j^i and v_j^o to record weight updates. CLE assumes that the updates to W_1^c and W_2^c do not alter the network. This assumption holds if the network's activation functions are piecewise linear (e.g. ReLU), and if the pair of layers have no skip connections in between.

AFCLE results in no real increase in parameter count, since the vectors v_j^i and v_j^o can be folded into W_j and b_j after data-free compression is completed. The advantages of AFCLE over CLE are (1) it can be used for activation functions that aren't piecewise linear, (2) it does not require special handling for skip connections (since any pair of layers can be equalized), and (3) it does not corrupt the BatchNorm [25] statistics needed for data generation. However, the usage of AFCLE for activations that aren't piecewise

linear is not well-motivated, since the theoretical analysis from [40] does not apply. In practice, the third advantage is the most important.

3.3. Data-Free Quantization

Our method quantizes both weights and activation ranges. As is standard, we set our weight quantizers to the minimum and maximum of the weight tensors [26]. Setting the activation quantizers is done in DFQ [40] by setting the maximum and minimum activation range to six standard deviations away from the mean, as determined by BatchNorm [25] statistics. The lower activation range is then clamped to 0, since ReLU [1] activations are used in their networks.

Instead, we set activation ranges by performing a simple optimization using generated data (Algorithm 1). Recall that the quantized version of a floating-point activation tensor X can be expressed as

$$k_b = \frac{h - l}{2^b - 1} \quad (13)$$

$$Q(X, l, h, b) = \left\lceil \frac{\min(\max(X, l), h) - l}{k_b} \right\rceil k_b + l, \quad (14)$$

where l is the minimum of the quantization range, h is the maximum, b is the number of bits in the quantization scheme, and $\lceil \cdot \rceil$ denotes rounding to the nearest integer. We perform a grid search jointly over $h \in [0, \max(X_{\max}, 0)]$ and $l \in [\min(0, X_{\min}), 0]$ to choose the h and l parameters that minimize $|X - Q(X, l, h, b)|_2$. Note that, when generating data using Algorithm 1, we also account for the scaling applied by the preceding v_j^o buffers (produced by AFCLE), to ensure data is of the correct scale, which is essential for setting quantization ranges.

Our full method is as follows: first, we perform BatchNorm fusion and AFCLE on the student network (Section 3.2). Then, we perform bias absorption, as in [40]. Next, we set activation quantizers (Algorithm 1). Then, we perform bias correction, as in [40]. We set activation quantizers again, because the bias correction step adjusted weights (and therefore output statistics) slightly. The final step is to account for the affect of v_j^i and v_j^o buffers produced by AFCLE, and set weight quantization ranges. We can fold these buffers into the weight buffers as described in Section 3.2. However, since we focus experimentation on ReLU networks and don't propagate AFCLE through skip connections (as described in Section 4, for closer comparison to [40]) we can simply discard them, since a layer's v_j^o buffer will be reversed by the following layer's v_j^i buffer.

3.4. Data-Free Pruning

We show how to use our method to construct a sparse student without any training data. We begin by recording

Algorithm 1: Computing Activation Quantizers

Input: input means μ_j , input standard deviations σ_j , input activation functions f_j (for $j \in \mathcal{K}$), number of steps N , quantization bits b
 $\mathcal{G}_{\mathcal{C}_i} = \sum_{j \in \mathcal{K}} f_j(\mathcal{N}(\mu_{\mathcal{B}_j}, \sigma_{\mathcal{B}_j}))$ (Equation 3)
 $d_{\max} \leftarrow \max(d), d_{\min} \leftarrow \min(d)$
 $h \leftarrow -\infty, l \leftarrow \infty, L \leftarrow \infty$
for $h_i \in [1, 2, \dots, N]$ **do**
 for $l_i \in [1, 2, \dots, N]$ **do**
 $\tilde{h} = (h_i/N) * (\max(d_{\max}, 0))$
 $\tilde{l} = (l_i/N) * (\min(d_{\min}, 0))$
 if $\|X - Q(X, \tilde{l}, \tilde{h}, b)\|_2 < L$ **then**
 $l \leftarrow \tilde{l}, h \leftarrow \tilde{h}$
 $L \leftarrow \|X - Q(X, \tilde{l}, \tilde{h}, b)\|_2$
 end if
 end for
end for
end for
return l, h

the BatchNorm statistics required for layer-wise data generation, as described in Section 3.1. We then perform fusion and AFCLE as a preprocessing step, as described in Section 3.2. We duplicate the resulting model to obtain a “teacher” and a “student”. For the remainder of our method, the teacher will remain unchanged, and the student will be pruned through data-free training.

We prune using Soft Threshold Reparameterization (STR) [30], which we review briefly. In the network's convolutional and fully-connected layers, an intermediate weight W_s is calculated as

$$W_s = \text{sign}(W) \cdot \text{ReLU}(|W| - \text{sigmoid}(s)), \quad (15)$$

where W is the weight tensor, and s is a model parameter used to control sparsity. This intermediate tensor W_s is used in place of W in the forward and pass. In the backward pass, the gradients are propagated to the original weight matrix W . A weight decay parameter λ is used to drive s upwards from an initial value $s_0 < 0$, which increases sparsity.

Let i be an index assigned to the convolutional or fully-connected layer \mathcal{C}_i^s in the student, and let the corresponding layer in the teacher (of the same architecture) be \mathcal{C}_i^t . Let $\mathcal{C}_i^s(\cdot)$ denote the application of layer s_i to an input tensor, and likewise for $\mathcal{C}_i^t(\cdot)$. Given a loss function L_i associated with layer i , we compute the loss for layer i as

$$L = L_i(\mathcal{C}_i^s(x), \mathcal{C}_i^t(x)), \quad (16)$$

where $x \sim \mathcal{G}_{\mathcal{C}_i^t}$ is generated from the expression in Equation 3. In our experiments, we choose L_i to be the mean square error loss for each i . We also freeze the student's bias during training, since our goal is to induce sparsity in

the weights. We empirically found that including the activations f_j in Equation 3 is not important during pruning, so we omit them from data generation for simplicity. After pruning, we simply fold the v_j^i and v_j^o buffers from AFCLE back into the original tensors.

4. Experiments

We provide results for data-free quantization and pruning on a variety of network architectures. We first show the results of our method compared to other computationally efficient methods. We then compare to computationally expensive generative methods requiring orders of magnitude more memory and runtime. We evaluate on ImageNet [9].

In all experiments (including baselines), teacher and student network weights are initialized to a pretrained model. We train in PyTorch [42] using NVIDIA Tesla V100 GPUs. For methods using backpropagation, we use Adam [27] with a cosine learning rate decaying from 0.001 to 0 over 10^5 iterations (though in practice, our method converges in only a few hundred iterations). For Adversarial Knowledge Distillation (AKD) [6], we use the training parameters in the original work. We use batch size 128 for all methods, reducing it to fit on a single GPU as needed. See Appendix for additional details on AKD and Deep Inversion [53].

When generating data for quantizing activations (Algorithm 1), we use a batch size of 2000, and optimize for $N = 100$ steps. To induce sparsity in models, we use STR [30]. We vary the s_0 value (which controls initial sparsity) between -2 and -7 in increments of 0.33. We fix the sparsity-inducing weight decay parameter to $\lambda = 0.00001551757813$, as in [30]. We do not apply this weight decay to the student’s weights since we want to allow the student’s weights to closely match the teacher.

In all MobileNetV2 [45] experiments, we replace ReLU6 with ReLU [1] as in DFQ [40]. The accuracy of this modified network is identical to that of the original network. When running our Assumption-Free Cross-Layer Equalization method, we don’t equalize across residual connections in MobileNetV2 and ResNet18, as in DFQ [40].

When reloading pretrained networks, our floating-point accuracies for our networks were 71.82% for MobileNetV1 1.0 [24], 64.95% for MobileNetV1 0.5 [24], 71.88% for MobileNetV2 [45], 69.76% for ResNet18, and 76.30% for EfficientNet B0 [48]. We restrict EfficientNet B0 experiments to pruning, because most of our quantization baselines do not apply to EfficientNet B0 (which contains non-ReLU activations [1]), and because preliminary experiments showed poor results for applicable baselines.

4.1. Data-Free Quantization

Efficient Quantization: In Table 1, we compare our results with methods with a similar compute envelope (see

Bits	ours	DFQ	AR	ours	DFQ	AR
				MNV1 1.0	MNV2	
8	71.13	71.18	71.35	70.50	70.16	68.61
7	70.26	69.76	70.22	69.67	68.89	66.65
6	66.95	61.81	63.68	66.97	63.06	51.00
5	55.37	25.63	29.17	56.33	23.41	27.83
4	5.62	0.23	0.28	8.23	0.49	0.48
MNV1 0.5				RN18		
8	63.77	63.65	56.39	68.67	67.72	56.24
7	61.64	60.47	51.01	67.92	66.40	54.45
6	55.51	44.67	34.44	63.72	62.86	50.57
5	23.79	7.29	5.48	35.47	34.76	43.64
4	1.71	0.24	0.28	0.88	1.06	10.64

Table 1. ImageNet results for computationally efficient quantization methods on MobileNetV1, MobileNetV2, and ResNet18. (DFQ): Data-Free Quantization [40]. (AR): AdaRound [39].

Bits	ours	AKD	DI	ours	AKD	DI
				MNV1 1.0	MNV2	
8	71.13	70.13	24.53	70.50	19.33	7.21
7	70.26	67.77	21.35	69.67	4.87	5.43
6	66.95	7.11	19.17	66.97	9.70	3.54
5	55.37	0.10	9.06	56.33	0.86	2.62
4	5.62	0.10	0.10	8.23	0.10	0.09
MNV1 0.5				RN18		
8	63.77	62.83	25.75	68.67	62.13	19.69
7	61.64	57.20	19.05	67.92	61.38	19.05
6	55.51	48.00	22.17	63.72	54.96	16.98
5	23.79	16.86	6.70	35.47	41.41	12.43
4	1.71	0.10	0.10	0.88	0.10	6.33

Table 2. Comparing our efficient method with computationally expensive quantization methods on MobileNetV1, MobileNetV2, and ResNet18 using ImageNet. (AKD): Adversarial Knowledge Distillation [6]. (DI): DeepInversion [6].

Figure 2). We compare to DFQ [40], which performs equalization, bias absorption, and bias correction on networks. We also compare to AdaRound [39], which performs equalization, then optimizes over rounding decisions. Note that the original method requires using data to collect activation statistics. To compare with data-free methods, we instead generate batches of data using the BatchNorm [25] statistics of the previous layer, using Equation 3.

Since our method and DFQ don’t require backpropagation, we simply report the accuracy. For AdaRound, which requires backpropagation, we report the final-epoch accuracy, since a truly data-free scenario would not allow for a validation set on which to perform early stopping. Our method achieves state-of-the-art accuracy in nearly all cases. Interestingly, we found that AdaRound accuracy de-

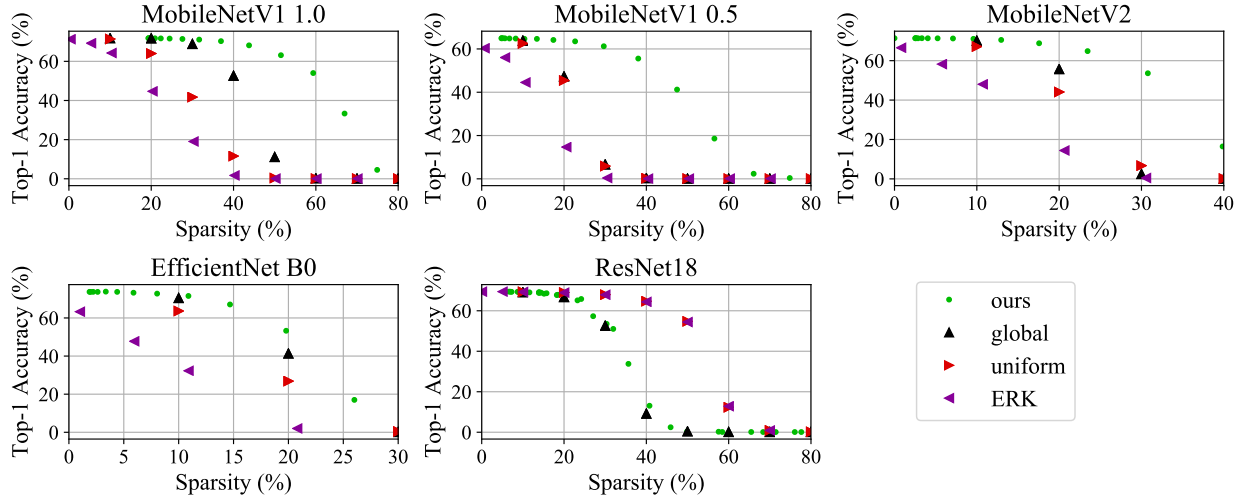


Figure 3. Comparison of our efficient pruning method to efficient baselines on ImageNet. (Global [5]): a global magnitude threshold is used to prune weights. (Uniform [5]): a uniform layer-wise sparsity budget is used. (ERK [13]): a layer-wise sparsity budget weighted to prune more weights from larger convolutional layers, as described in Equation 17.

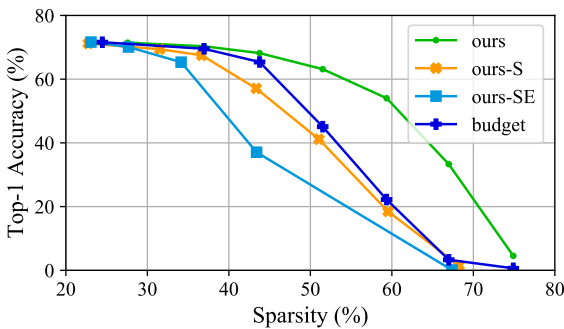


Figure 4. Ablation study of our pruning method on MobileNetV1.0 on ImageNet. (Ours-S): our method, but using data generated from $\mathcal{N}(0, 1)$, rather than from BatchNorm statistics. (Ours-SE): our method, with data generated from $\mathcal{N}(0, 1)$, and without AFCLE. (Budget): a model using the layer-wise pruning budget learned by our method, but without training the weights.

creases with training in a few low-bit-width scenarios. See Appendix for analysis.

Expensive Quantization: We evaluate the results of computationally expensive methods in Table 2. When training with images generated using DeepInversion (DI) [53], we use the Label Refinery [2] formulation for Knowledge Distillation [23]. See Appendix for additional details on experimental setup for AKD and DI.

Our method outperforms these generative methods at a fraction of the computational cost (Figure 2). As before, we provide final epoch accuracy. We found that DI had difficulty providing an effective training signal to a quantized student. The adaptive nature of AKD, which uses a Generative Adversarial Network (GAN), proved more effective.

However, training the GAN suffered from stability issues in some cases. For example, our results for 6-bit quantization of ‘‘MN1 1.0’’ were surpassed by ‘‘MN1 0.5’’, which is unexpected. In fact, the accuracy of ‘‘MN1 1.0’’ at 6 bits is high in early training iterations, but decreases due to instability. See Appendix for analysis.

4.2. Data-Free Pruning

Efficient Pruning: We present our results for our pruning method in Figure 3. We compare our final-epoch accuracy against three baselines. The ‘‘global’’ baseline corresponds to pruning every weight whose magnitude is smaller than a given threshold [5]. The ‘‘uniform’’ baseline corresponds to applying a uniform sparsity level to each layer by pruning the weights with smallest magnitude [5]. The Erdos-Renyi Kernel (ERK) baseline corresponds to a budgeted layer-wise pruning suggested in RigL [13]. Each layer’s number of pruned weights is proportional to

$$p = \frac{c_o + c_i + k_h + k_w}{c_o * c_i * k_h * k_w}, \quad (17)$$

where c_o is the number of output dimensions, c_i is the number of input dimensions, and k_h, k_w are the kernel height and width. For these three baselines, we perform Batch-Norm fusion (for reasons described in Section 3.2) because it is a standard technique, but we do not perform AFCLE (since it is part of our method). These methods are essentially free, and are omitted from the analysis in Figure 2.

Our method outperforms our baselines for achieving efficient, data-free sparsity in all cases except ResNet18. ResNet18 is overparameterized by comparison to the other architectures, so the uniform pruning method is able to re-

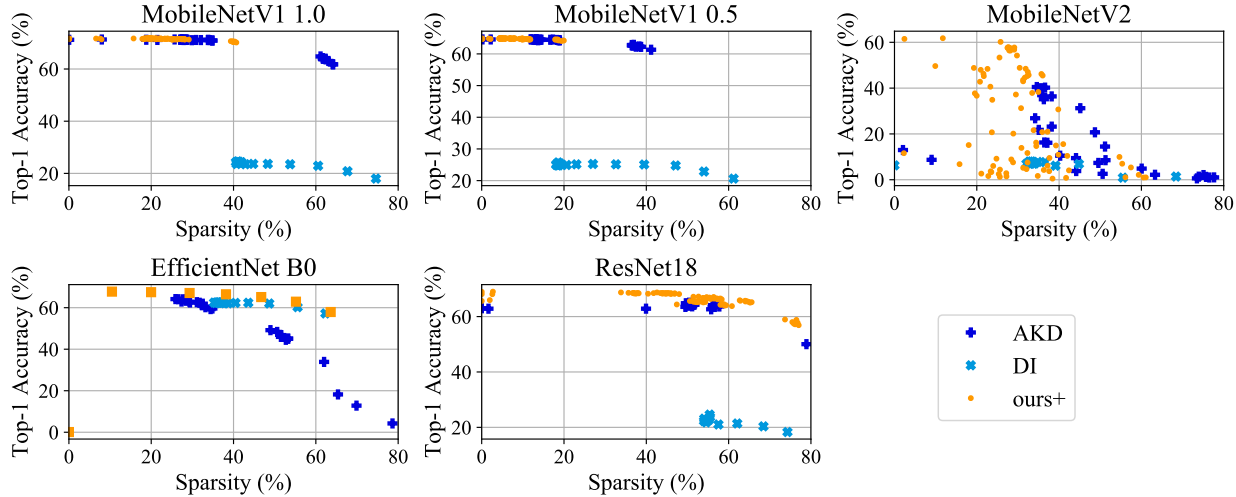


Figure 5. Comparison of computationally expensive pruning methods on ImageNet. We take the best-performing method for each network (e.g. DI [53] for EfficientNet B0 and AKD [6] for the others) and combine it with our loss to yield “ours+”. We plot the final-epoch accuracy of training jobs. In the case of MobileNetV2, AKD is not very stable, including when combined with our method.

move up to 40% of its weights before incurring large accuracy losses. We find our method is more effective for pruning all other architectures.

In Figure 4, we present an ablation of our method. We find that both AFCLE and the usage of BatchNorm statistics for data generation contribute to our sparsity/accuracy tradeoff. Additionally, our method learns a sparsity budget that outperforms the baseline methods (“budget”, Figure 4).

Expensive Pruning: We present results comparing our method to more computationally expensive methods, Adversarial Knowledge Distillation (AKD) [6] and Deep Inversion (DI) [53]. These methods involve generating end-to-end training data. We found we needed to sweep across more values of the sparsity-controlling weight decay parameter λ to encourage varying levels of sparsity in AKD. See Appendix for details. Again, we report final-epoch accuracy of models, since a data-free scenario does not allow for model selection using a validation set.

We found mixed results when using these computationally expensive methods. For all networks except EfficientNet B0, DI failed to produce solutions with more than 30% accuracy, which has limited practical value. For AKD, performance was stronger in general, although solutions for MobileNetV2 did not exceed 40% accuracy. Moreover, some parameter settings for MobileNetV2 resulted in very poor performance, even at low sparsity.

For each network, we combine our method with the top-performing method for that network (“ours+”, Figure 5). To do this, we add our loss to the loss function and backpropagate as usual. For ResNet18 and EfficientNet B0, we improve the accuracy/sparsity tradeoff. For MobileNetV2, we recover higher-accuracy solutions, improving the practical

usefulness of pruned models. For MobileNetV1, our results are similar to those produced by AKD.

Although these results achieve a stronger sparsity/accuracy tradeoff than the computationally efficient pruning results (Figure 3), we emphasize that getting these methods to work may be difficult in practice when no data is present. The AKD and DI methods contain many more hyperparameters than other methods. Parameters for AKD control the optimization procedure of the GAN, and parameters for DI control the image generation optimization. In general, these parameters vary with network architecture. Although we use settings presented in [6] and [53], these parameters may need more tuning to work on data from another domain, or for other architectures. Moreover, it was difficult to achieve a wide spread of models in the sparsity/accuracy manifold; for example, AKD and DI did not achieve above 40% accuracy on MobileNetV2. By contrast, the computationally inexpensive models can always achieve near-perfect accuracy (sometimes at more modest sparsity).

5. Conclusion

We present an efficient, effective method for data-free compression. We break this problem into the subproblem of compressing individual layers without data. We apply a novel equalization scheme to precondition networks to better maintain accuracy during compression. Then, we compress individual layers using data generated from BatchNorm [25] statistics from previous layers. Our method produces state-of-the-art results for quantization regardless of computational cost. Our method outperforms other computationally efficient methods for pruning, and can be combined with expensive methods to improve their results.

References

[1] Raman Arora, Amitabh Basu, Poorya Mianjy, and Anirbit Mukherjee. Understanding deep neural networks with rectified linear units. In *International Conference on Learning Representations*, 2018.

[2] Hessam Bagherinezhad, Maxwell Horton, Mohammad Rastegari, and Ali Farhadi. Label refinery: Improving imagenet classification through label progression. *CoRR*, abs/1805.02641, 2018.

[3] Guillaume Bellec, David Kappel, Wolfgang Maass, and Robert Legenstein. Deep rewiring: Training very sparse deep networks. In *International Conference on Learning Representations*, 2018.

[4] Aishwarya Bhandare, V. Sripathi, Deepthi Karkada, Vivek Menon, Sun Choi, Kushal Datta, and V. Saletore. Efficient 8-bit quantization of transformer neural machine language translation model. *ArXiv*, abs/1906.00532, 2019.

[5] Davis Blalock, Jose Javier Gonzalez Ortiz, Jonathan Franke, and John Guttag. What is the state of neural network pruning?, 2020.

[6] Yoojin Choi, Jihwan Choi, Mostafa El-Khamy, and Jungwon Lee. Data-free network quantization with adversarial knowledge distillation. In *Proceedings of the IEEE/CVF Conference on Computer Vision and Pattern Recognition (CVPR) Workshops*, June 2020.

[7] Matthieu Courbariaux and Yoshua Bengio. Binarynet: Training deep neural networks with weights and activations constrained to +1 or -1. *CoRR*, abs/1602.02830, 2016.

[8] Yann Le Cun, John S. Denker, and Sara A. Solla. Optimal brain damage. In *Advances in Neural Information Processing Systems*, pages 598–605. Morgan Kaufmann, 1990.

[9] J. Deng, W. Dong, R. Socher, L.-J. Li, K. Li, and L. Fei-Fei. ImageNet: A Large-Scale Hierarchical Image Database. In *CVPR09*, 2009.

[10] Tim Dettmers and Luke Zettlemoyer. Sparse networks from scratch: Faster training without losing performance, 2019.

[11] Giuseppe Di Guglielmo, Javier Mauricio Duarte, Philip Harris, Duc Hoang, Sergo Jindariani, Edward Kreinar, Mia Liu, Vladimir Loncar, Jennifer Ngadiuba, Kevin Pedro, and et al. Compressing deep neural networks on fpgas to binary and ternary precision with hls4ml. *Machine Learning: Science and Technology*, Jun 2020.

[12] Xin Dong, Shangyu Chen, and Sinno Jialin Pan. Learning to prune deep neural networks via layer-wise optimal brain surgeon. In *Proceedings of the 31st International Conference on Neural Information Processing Systems*, NIPS’17, page 4860–4874, Red Hook, NY, USA, 2017. Curran Associates Inc.

[13] Erich Elsen, Pablo Samuel Castro Rivadeneira, Trevor Gale, and Utku Evci. Rigging the lottery: Making all tickets winners. In *International Conference of Machine Learning*, 2020.

[14] Ruihao Gong, Xianglong Liu, Shenghu Jiang, Tianxiang Li, Peng Hu, Jiazhen Lin, Fengwei Yu, and Junjie Yan. Differentiable soft quantization: Bridging full-precision and low-bit neural networks. In *Proceedings of the IEEE/CVF International Conference on Computer Vision (ICCV)*, October 2019.

[15] Ian J. Goodfellow, Jean Pouget-Abadie, Mehdi Mirza, Bing Xu, David Warde-Farley, Sherjil Ozair, Aaron Courville, and Yoshua Bengio. Generative adversarial nets. In *Proceedings of the 27th International Conference on Neural Information Processing Systems - Volume 2*, NIPS’14, page 2672–2680, Cambridge, MA, USA, 2014. MIT Press.

[16] Hui Guan, Xipeng Shen, and Seung-Hwan Lim. Wootz: A compiler-based framework for fast cnn pruning via compositionality. In *Proceedings of the 40th ACM SIGPLAN Conference on Programming Language Design and Implementation*, PLDI 2019, page 717–730, New York, NY, USA, 2019. Association for Computing Machinery.

[17] Yiwen Guo, Anbang Yao, and Yurong Chen. Dynamic network surgery for efficient dnns. In *Proceedings of the 30th International Conference on Neural Information Processing Systems*, NIPS’16, page 1387–1395, Red Hook, NY, USA, 2016. Curran Associates Inc.

[18] Hai Victor Habi, Roy H. Jennings, and Arnon Netzer. Hmq: Hardware friendly mixed precision quantization block for cnns, 2020.

[19] Song Han, Jeff Pool, John Tran, and William Dally. Learning both weights and connections for efficient neural network. In C. Cortes, N. Lawrence, D. Lee, M. Sugiyama, and R. Garnett, editors, *Advances in Neural Information Processing Systems*, volume 28. Curran Associates, Inc., 2015.

[20] Matan Haroush, Itay Hubara, Elad Hoffer, and Daniel Soudry. The knowledge within: Methods for data-free model compression. In *Proceedings of the IEEE/CVF Conference on Computer Vision and Pattern Recognition (CVPR)*, June 2020.

[21] Babak Hassibi, David Stork, and Gregory Wolff. Optimal brain surgeon: Extensions and performance comparisons. In J. Cowan, G. Tesauro, and J. Alspector, editors, *Advances in Neural Information Processing Systems*, volume 6, pages 263–270. Morgan-Kaufmann, 1994.

[22] Kaiming He, Xiangyu Zhang, Shaoqing Ren, and Jian Sun. Deep residual learning for image recognition. In *Proceedings of the IEEE Conference on Computer Vision and Pattern Recognition (CVPR)*, June 2016.

[23] Geoffrey Hinton, Oriol Vinyals, and Jeffrey Dean. Distilling the knowledge in a neural network. In *NIPS Deep Learning and Representation Learning Workshop*, 2015.

[24] A. Howard, Menglong Zhu, Bo Chen, D. Kalenichenko, W. Wang, Tobias Weyand, M. Andreetto, and H. Adam. Mobilenets: Efficient convolutional neural networks for mobile vision applications. *ArXiv*, abs/1704.04861, 2017.

[25] Sergey Ioffe and Christian Szegedy. Batch normalization: Accelerating deep network training by reducing internal covariate shift. In *Proceedings of the 32nd International Conference on International Conference on Machine Learning - Volume 37*, ICML’15, page 448–456. JMLR.org, 2015.

[26] Benoit Jacob, Skirmantas Kligys, Bo Chen, Menglong Zhu, Matthew Tang, Andrew Howard, Hartwig Adam, and Dmitry Kalenichenko. Quantization and training of neural networks for efficient integer-arithmetic-only inference. In *Proceed-*

ings of the IEEE Conference on Computer Vision and Pattern Recognition (CVPR), June 2018.

[27] Diederik P. Kingma and Jimmy Ba. Adam: A method for stochastic optimization. In Yoshua Bengio and Yann LeCun, editors, *3rd International Conference on Learning Representations, ICLR 2015, San Diego, CA, USA, May 7-9, 2015, Conference Track Proceedings*, 2015.

[28] Raghuraman Krishnamoorthi. Quantizing deep convolutional networks for efficient inference: A whitepaper. *CoRR*, abs/1806.08342, 2018.

[29] Alex Krizhevsky, Ilya Sutskever, and Geoffrey E Hinton. Imagenet classification with deep convolutional neural networks. In *Advances in neural information processing systems*, pages 1097–1105, 2012.

[30] Aditya Kusupati, Vivek Ramanujan, Raghav Somani, Mitchell Wortsman, Prateek Jain, Sham Kakade, and Ali Farhadi. Soft threshold weight reparameterization for learnable sparsity. In *Proceedings of the International Conference on Machine Learning*, July 2020.

[31] Namhoon Lee, Thalaiyasingam Ajanthan, and Philip Torr. SNIP: SINGLE-SHOT NETWORK PRUNING BASED ON CONNECTION SENSITIVITY. In *International Conference on Learning Representations*, 2019.

[32] R. Li, Y. Wang, F. Liang, H. Qin, J. Yan, and R. Fan. Fully quantized network for object detection. In *2019 IEEE/CVF Conference on Computer Vision and Pattern Recognition (CVPR)*, pages 2805–2814, 2019.

[33] Mingbao Lin, Rongrong Ji, Shaojie Li, Qixiang Ye, Yonghong Tian, J. Liu, and Q. Tian. Filter sketch for network pruning. *ArXiv*, abs/2001.08514, 2020.

[34] Bin Liu, Yue Cao, Mingsheng Long, Jianmin Wang, and Jingdong Wang. Deep triplet quantization. In *Proceedings of the 26th ACM International Conference on Multimedia, MM ’18*, page 755–763, New York, NY, USA, 2018. Association for Computing Machinery.

[35] Christos Louizos, Max Welling, and Diederik P. Kingma. Learning sparse neural networks through l_0 regularization. In *International Conference on Learning Representations*, 2018.

[36] Brais Martinez, Jing Yang, Adrian Bulat, and Georgios Tzimiropoulos. Training binary neural networks with real-to-binary convolutions. In *International Conference on Learning Representations*, 2020.

[37] H. Brendan McMahan, Eider Moore, Daniel Ramage, and Blaise Agüera y Arcas. Federated learning of deep networks using model averaging. *CoRR*, abs/1602.05629, 2016.

[38] Eldad Meller, Alexander Finkelstein, Uri Almog, and Mark Grobman. Same, same but different: Recovering neural network quantization error through weight factorization. In Kamalika Chaudhuri and Ruslan Salakhutdinov, editors, *Proceedings of the 36th International Conference on Machine Learning*, volume 97 of *Proceedings of Machine Learning Research*, pages 4486–4495. PMLR, 09–15 Jun 2019.

[39] M. Nagel, Rana Ali Amjad, Mart van Baalen, Christos Louizos, and Tijmen Blankevoort. Up or down? adaptive rounding for post-training quantization. *ArXiv*, abs/2004.10568, 2020.

[40] Markus Nagel, Mart van Baalen, Tijmen Blankevoort, and Max Welling. Data-free quantization through weight equalization and bias correction. In *Proceedings of the IEEE/CVF International Conference on Computer Vision (ICCV)*, October 2019.

[41] Sharan Narang, Greg Diamos, S. Sengupta, and E. Elsen. Exploring sparsity in recurrent neural networks. *ArXiv*, abs/1704.05119, 2017.

[42] Adam Paszke, Sam Gross, Francisco Massa, Adam Lerer, James Bradbury, Gregory Chanan, Trevor Killeen, Zeming Lin, Natalia Gimelshein, Luca Antiga, Alban Desmaison, Andreas Kopf, Edward Yang, Zachary DeVito, Martin Raison, Alykhan Tejani, Sasank Chilamkurthy, Benoit Steiner, Lu Fang, Junjie Bai, and Soumith Chintala. Pytorch: An imperative style, high-performance deep learning library. In H. Wallach, H. Larochelle, A. Beygelzimer, F. d’Alché-Buc, E. Fox, and R. Garnett, editors, *Advances in Neural Information Processing Systems 32*, pages 8024–8035. Curran Associates, Inc., 2019.

[43] Mohammad Rastegari, Vicente Ordonez, Joseph Redmon, and Ali Farhadi. Xnor-net: Imagenet classification using binary convolutional neural networks. In *European Conference on Computer Vision*, pages 525–542. Springer, 2016.

[44] Joseph Redmon and Ali Farhadi. Yolo9000: Better, faster, stronger. In *Computer Vision and Pattern Recognition (CVPR), 2017 IEEE Conference on*, pages 6517–6525. IEEE, 2017.

[45] Mark Sandler, Andrew Howard, Menglong Zhu, Andrey Zhmoginov, and Liang-Chieh Chen. Mobilenetv2: Inverted residuals and linear bottlenecks. In *Proceedings of the IEEE Conference on Computer Vision and Pattern Recognition (CVPR)*, June 2018.

[46] Suraj Srinivas and R. Venkatesh Babu. Data-free parameter pruning for deep neural networks. In *BMVC*, 2015.

[47] X. Suau, u. Zappella, and N. Apostoloff. Filter distillation for network compression. In *2020 IEEE Winter Conference on Applications of Computer Vision (WACV)*, pages 3129–3138, 2020.

[48] Mingxing Tan and Quoc Le. EfficientNet: Rethinking model scaling for convolutional neural networks. In Kamalika Chaudhuri and Ruslan Salakhutdinov, editors, *Proceedings of the 36th International Conference on Machine Learning*, volume 97 of *Proceedings of Machine Learning Research*, pages 6105–6114. PMLR, 09–15 Jun 2019.

[49] Mitchell Wortsman, Ali Farhadi, and Mohammad Rastegari. Discovering neural wirings. In H. Wallach, H. Larochelle, A. Beygelzimer, F. d’Alché-Buc, E. Fox, and R. Garnett, editors, *Advances in Neural Information Processing Systems*, volume 32, pages 2684–2694. Curran Associates, Inc., 2019.

[50] Hao Wu, P. Judd, Xiaojie Zhang, M. Isaev, and P. Micikevicius. Integer quantization for deep learning inference: Principles and empirical evaluation. *ArXiv*, abs/2004.09602, 2020.

[51] Shoukai Xu, Haokun Li, Bohan Zhuang, Jing Liu, Jiezhang Cao, Chuangrun Liang, and Mingkui Tan. Generative low-bitwidth data free quantization. In Andrea Vedaldi, Horst Bischof, Thomas Brox, and Jan-Michael Frahm, editors,

Computer Vision – ECCV 2020, Lecture Notes in Computer Science, pages 1–17. Springer, 2020. European Conference on Computer Vision 2020, ECCV 2020 ; Conference date: 23-08-2020 Through 28-08-2020.

- [52] Y. Yang, Shuang Wu, Lei Deng, Tianyi Yan, Yuan Xie, and Guoqi Li. Training high-performance and large-scale deep neural networks with full 8-bit integers. *Neural networks : the official journal of the International Neural Network Society*, 125:70–82, 2020.
- [53] Hongxu Yin, Pavlo Molchanov, Jose M. Alvarez, Zhizhong Li, Arun Mallya, Derek Hoiem, Niraj K Jha, and Jan Kautz. Dreaming to distill: Data-free knowledge transfer via deep-inversion. In *The IEEE/CVF Conf. Computer Vision and Pattern Recognition (CVPR)*, June 2020.

A. Note on Quantization With Residuals

When quantizing a network with residual connections, one must take care to ensure that the activation tensor created by adding the output of quantized convolutions is quantized *after* the addition from the residual is applied. Otherwise, the input to the following layer will not be truly quantized.

To ensure this, we place our activation quantization modules after the skip connections in the case of residual networks. In our DFQ [40] implementation, we need batch norm input statistics for the layer following a skip connection. It is not clear from the discussion in [40] where their activation modules are, or how this detail is handled. When estimating statistics needed for the output of the skip connections (which is needed for DFQ), we estimate the per-channel output statistics from a skip connection as $\mu = \mu_1 + \mu_2$, $\sigma = \sqrt{\sigma_1^2 + \sigma_2^2}$, where μ_i, σ_i are the mean and standard deviation of the batch norm statistics from the inputs to the residual addition.

B. Notes on Experimental Setup

We note here a few details of our experimental setup for Adversarial Knowledge Distillation (AKD) [6] and Deep Inversion (DI) [53].

When using DI to generate data for MobileNet, MobileNetV2, ResNet18, and EfficientNet B0, we use the parameters for MobileNetV2 [45] from the public GitHub repository (settings for these other networks were not in the repository). We validated that these settings generated images that could be recognized by an independent CNN as belonging to the given class. As in [53], we generate 165,000 images and use them to retrain a student network from a teacher network. We initialize both the student and the teacher to the same pretrained network. We then train the student with STR [30] to match the teacher using the Label Refinery [2] formulation for Knowledge Distillation [23]. We train for 10 epochs over this training set, using Adam [27] with a cosine learning rate decaying from 0.001 to 0.

When training with AKD [6], we use the parameter settings described in [6]. Specifically, we trained the discriminator with Nesterov gradient descent with momentum 0.9 and initial learning rate 0.1. We used Adam [27] to optimize the generator, with an initial learning rate 0.001. We decay both learning rates to 0 over the course of training, using a cosine learning rate schedule. We use a loss-scaling alpha of $\alpha = 0.1$ (see [6] for details). We adjusted batch sizes to fit in a single NVIDIA Tesla V100 for all experiments. We initialized the student and teacher networks to the same pretrained model, then trained to produce a quantized or sparse model. Since we reloaded pretrained students and teachers, we found we could shorten the training regime and still

reach convergence. Optimizing the training regime is important for fair runtime comparison in Figure 2. Our epochs in this case were shortened to 12800 samples, and we perform warmup for 50 epochs (enough to plateau the generator loss) and regular training for 250 epochs (enough to reach convergence in all cases).

When training to induce sparsity with AKD, we found it important to adjust the sparsity-inducing weight decay λ (see STR [30] for details). In addition to setting $\lambda = 0.00001551757813$ (as for our other experiments), we used values of 2λ , 10λ , and 100λ to achieve a richer variety of points on the sparsity/accuracy trade-off curve. We found this important in practice. However, in the data-free scenario, we would not in general have access to a validation set, so we show all final-epoch results in Figure 2. We also found it useful to adjust our sweep over s_0 values to values that induce an initial sparsity of $[0\%, 10\%, \dots, 70\%]$.

When combining our method with DeepInversion (for EfficientNet B0) in Figure 5, we simply add our loss to the DeepInversion loss. When combining our method with AKD (for MobileNetV1, MobileNetV2, and ResNet18) in Figure 5, we scale our loss by factors of $[0.1, 1, 10, 100]$, add it to the discriminator loss, and plot all final-epoch results.

C. Analysis of Stability in Quantized Methods

We present the results for best-epoch performance (rather than last-epoch performance) of efficient quantization methods in Table 3. Since only AdaRound [39] requires backpropagation, only the AdaRound entries are different than the last-epoch results in Table 1. The results for DFQ [40] and our method are unchanged. Results for best-epoch performance of expensive quantization methods appear in Table 4. Note that these best-epoch results give an unrealistic advantage to AdaRound [39], Adversarial Knowledge Distillation [6], and Deep Inversion [53], because a data-free scenario would not allow for a validation set in practice.

Note that gains are modest in some cases, but very large in other cases. We noticed that in some cases (*e.g.* ResNet18), AdaRound accuracy actually decreases with training, indicating that the preprocessing step provided reasonably accurate quantization, but the training step introduced instability. Additionally, 6-bit MobileNetV1 1.0 achieved a lower final-epoch accuracy than 6-bit MobileNetV1 0.5 (Table 2) when using Adversarial Knowledge Distillation (AKD). In Table 4, we see that the best-epoch accuracy of MobileNetV1 1.0 was much higher than MobileNetV1 0.5 when using AKD. Instability in the optimization lead to the poor final-epoch results in Table 2 for 6-bit MobileNetV1 1.0 with AKD.

Bits	ours	DFQ		AR		ours	DFQ		AR	
		MNV1 1.0		MNV2			MNV2		RN18	
8	71.13	71.18	71.36 (+0.01)	70.50	70.16	69.73 (+1.12)				
7	70.26	69.76	70.27 (+0.05)	69.67	68.89	68.65 (+2.00)				
6	66.95	61.81	64.28 (+0.60)	66.97	63.06	51.93 (+0.93)				
5	55.37	25.63	29.17 (+0.00)	56.33	23.41	27.83 (+0.00)				
4	5.62	0.23	0.30 (+0.02)	8.23	0.49	0.51 (+0.03)				
MNV1 0.5					RN18					
8	63.77	63.65	62.18 (+5.79)	68.67	67.72	67.64 (+11.40)				
7	61.64	60.47	53.71 (+2.70)	67.92	66.40	66.78 (+12.33)				
6	55.51	44.67	35.42 (+0.98)	63.72	62.86	62.49 (+11.92)				
5	23.79	7.29	6.02 (+0.54)	35.47	34.76	51.53 (+7.89)				
4	1.71	0.24	0.31 (+0.03)	0.88	1.06	11.15 (+0.51)				

Table 3. Results for computationally-efficient quantization methods on MobileNetV1, MobileNetV2, and ResNet18 on ImageNet. This presents the results in Table 1, but showing the best epoch (rather than last epoch) for AR. The difference between the best epoch and the last epoch is reported in parenthesis. As our method and DFQ do not require backpropagation, the results are the same as in Table 1. (DFQ): Data-Free Quantization [40]. (AR): AdaRound [39].

Bits	ours	AKD		DI		ours	AKD		DI	
		MNV1 1.0		MNV2			MNV2		RN18	
8	71.13	70.31 (+0.18)	24.77 (+0.24)	70.50	19.57 (+0.24)	7.21 (+0.00)				
7	70.26	68.16 (+0.39)	25.00 (+3.65)	69.67	5.15 (+0.28)	5.60 (+0.17)				
6	66.95	61.38 (+54.27)	19.24 (+0.07)	66.97	10.05 (+0.35)	3.65 (+0.11)				
5	55.37	31.59 (+31.49)	9.06 (+0.00)	56.33	2.08 (+1.22)	2.62 (+0.00)				
4	5.62	0.10 (+0.00)	0.10 (+0.00)	8.23	0.10 (+0.00)	0.16 (+0.07)				
MNV1 0.5					RN18					
8	63.77	63.28 (+0.45)	27.98 (+2.23)	68.67	62.27 (+0.14)	20.16 (+0.47)				
7	61.64	60.11 (+2.91)	27.10 (+8.05)	67.92	61.39 (+0.01)	19.14 (+0.09)				
6	55.51	52.16 (+4.16)	22.58 (+0.41)	63.72	55.22 (+0.26)	17.50 (+0.52)				
5	23.79	21.18 (+4.32)	6.70 (+0.00)	35.47	41.41 (+0.00)	12.43 (+0.00)				
4	1.71	0.10 (+0.00)	0.10 (+0.00)	0.88	0.10 (+0.00)	6.62 (+0.29)				

Table 4. Results for our efficient method compared to computationally-expensive quantization methods on MobileNetV1, MobileNetV2, and ResNet18 on ImageNet. This presents the results in Table 2, but showing the best epoch (rather than last epoch) for AKD and DI. The difference between the best epoch and the last epoch is reported in parenthesis. As our method does not require backpropagation, the results are the same as in Table 2. (AKD): Adversarial Knowledge Distillation [6]. (DI): DeepInversion [6].

D. Loss and Accuracy Correlation

We also investigate the correlation between the loss function and the accuracy of methods. This correlation is of particular interest in data-free compression, because if no data is available, it's likely that no validation set is available. In this case, we may need to judge the relative quality of a variety of models by examining their loss values.

We show the correlation between training loss and validation accuracy for quantization methods in Figure 6. Since DFQ does not specify a method for determining the loss, we omit it. For our method, the loss is represented by the sum of squared differences between our generated activations and the quantized activations during our first round of activation quantization (see Section 4.1). For all other

methods, we report training loss. When reporting the loss for AKD, we ignore the generator loss, since the generator loss is not directly used to train the compressed student. For ease of visualization, we normalize the losses to fall in $[0, 1]$ for the given training jobs. We normalize model accuracies by the accuracy of the original floating-point model from which we reloaded our weights.

We find that loss and accuracy are correlated. When using our method or AdaRound, a lower loss always corresponds to a higher accuracy. For AKD and DI, the trend generally holds, but with at least one exception.

In Figure 7, we compare the loss and accuracies of our pruning method compared to DI [53], AKD [6], and “ours+”. Since the “global,” “uniform,” and “ERK” methods do not specify a method for calculating the loss, we

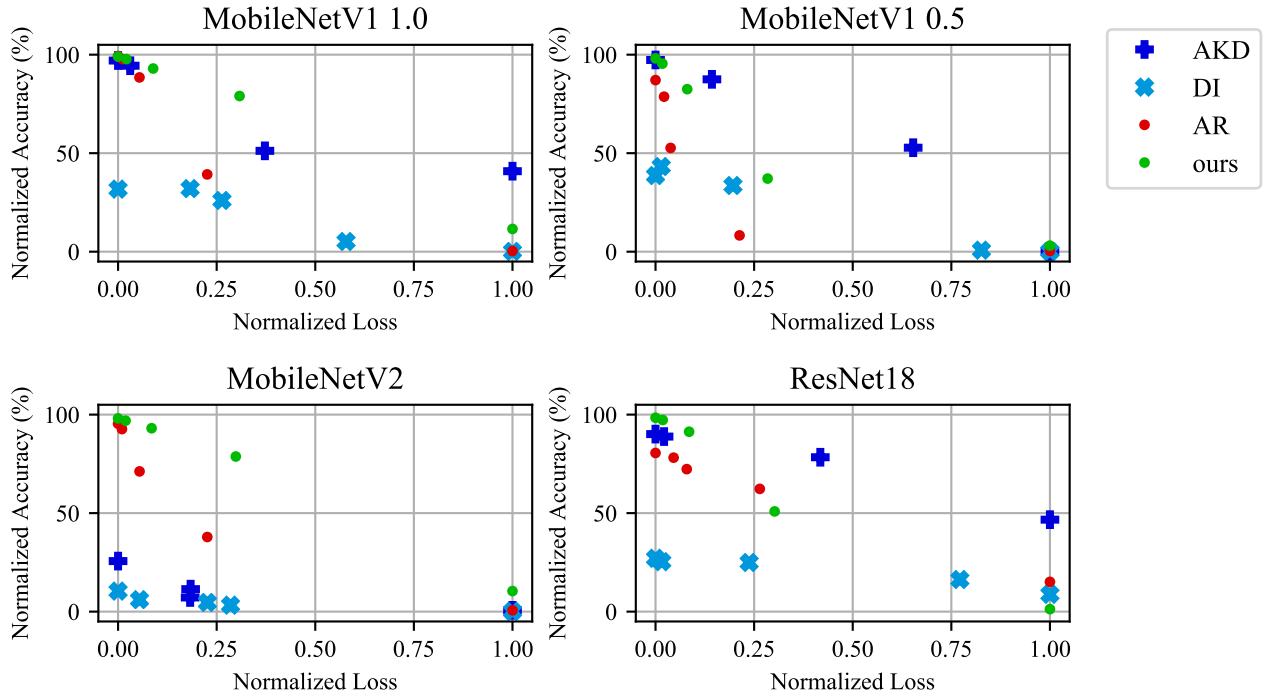


Figure 6. Correlation between normalized training loss and normalized validation accuracy on ImageNet for quantization methods.

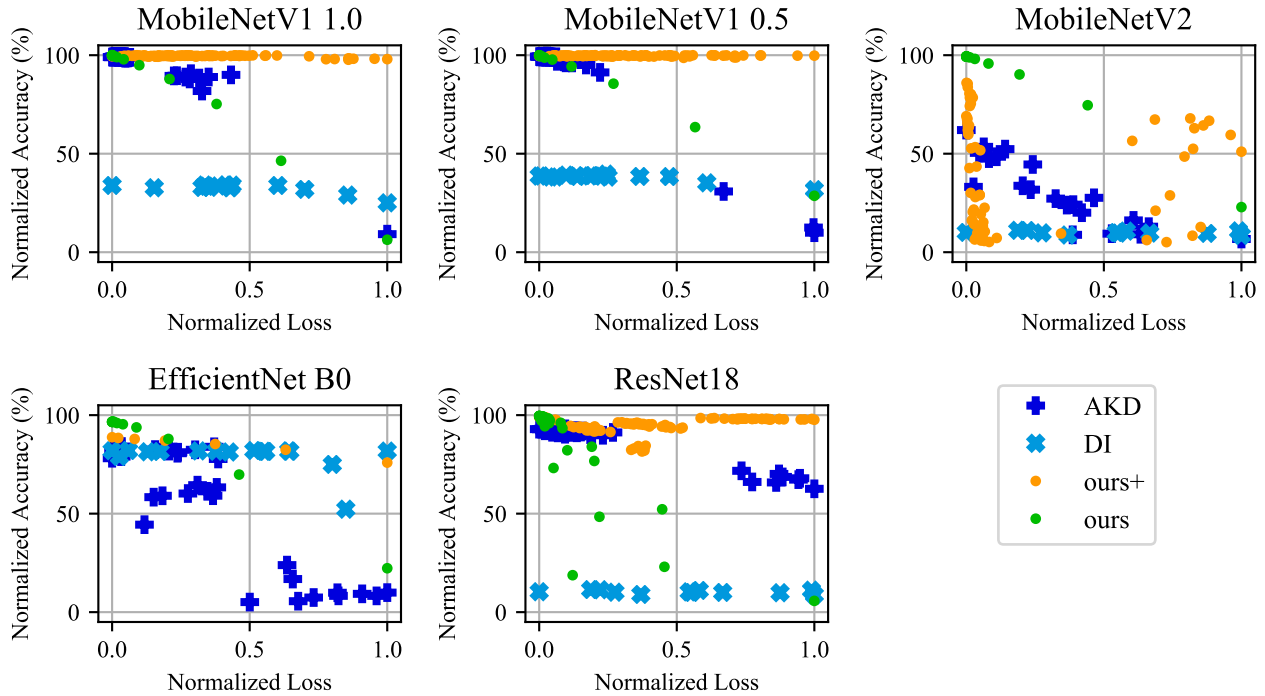


Figure 7. Correlation between normalized training loss and normalized validation accuracy on ImageNet for pruning methods.

omit them. Recall that “ours+” represents combining our method with DI for EfficientNet B0, and represents combining our method with AKD for all other networks. We show final-epoch accuracies and losses for jobs that have a final-epoch accuracy of at least 5%. We ignore jobs with lower accuracy for better visualization, because some loss functions are unbounded for models that achieve very poor accuracy. Note that, when reporting the loss for AKD, we again ignore the generator loss. As before, we normalize losses to fall in $[0, 1]$, and we normalize model accuracies by the accuracy of the original floating-point model from which we reload.

We find our method typically exhibits a strong loss/accuracy correlation. The noisiest example is ResNet18, in which some models achieve poor accuracy at relatively low loss. With our method, we are also always able to reproduce near-original model accuracy at a low loss. The AKD, DI, and “ours+” methods generally show a trend of higher accuracy when loss is lower, though some exceptions break the pattern. For MobileNetV1 1.0 and MobileNetV1 0.5, the “ours+” method never produces low-accuracy solutions, so increased loss does not show a decrease in accuracy, simply because low-accuracy solutions were not found.